AGU Advances

RESEARCH ARTICLE
10.1029/2021AV000407

Peer Review The peer review history for this article is available as a PDF in the Supporting Information.

Key Points:

- Smartphones used in a fixed network can provide earthquake early warning performance similar to scientific-grade instrumentation. Operating in Costa Rica over 6 months, the Alerta Sismica Temprana Utilizando Teléfonos Inteligentes (Earthquake Early Warning Utilizing Smartphones) project detected five events that caused wide-spread felt shaking and had zero false alarms
- The detections and alerts would have provided time for drop-cover-hold-on protective actions to be taken before *S*-wave arrival for large percentages of the Costa Rican population
- Two of the five events were triggered by *P*-waves on the phones, suggesting that smartphone-based earthquake early warning could be more effective than previously thought

Supporting Information:

Supporting Information may be found in the online version of this article.

Correspondence to:

B. A. Brooks,
bbrooks@usgs.gov

Citation:

Brooks, B. A., Protti, M., Ericksen, T., Bunn, J., Vega, F., Cochran, E. S., et al. (2021). Robust earthquake early warning at a fraction of the cost: ASTUTI Costa Rica. *AGU Advances*, *2*, e2021AV000407. https://doi.org/10.1029/2021AV000407

Robust Earthquake Early Warning at a Fraction of the Cost: ASTUTI Costa Rica

Benjamin A. Brooks[1], Marino Protti[2], Todd Ericksen[1], Julian Bunn[3], Floribeth Vega[2], Elizabeth S. Cochran[4], Chris Duncan[5], Jon Avery[6], Sarah E. Minson[1], Esteban Chaves[2], Juan Carlos Baez[7], James Foster[6], and Craig L. Glennie[8]

[1]Earthquake Science Center, US Geological Survey, Moffet Field, CA, USA, [2]Observatorio Vulcanologico y Sismologico de Costa Rica Campus Omar Dengo, Heredia, Costa Rica, [3]Center for Data Driven Discovery, California Institute of Technology, Pasadena, CA, USA, [4]Earthquake Science Center, US Geological Survey, Pasadena, CA, USA, [5]GISmatters, Amherst, MA, USA, [6]Hawaii Institute for Geophysics and Planetology, School of Ocean and Earth Science and Technology, University of Hawai'i, Honolulu, HI, USA, [7]Centro Sismologico Nacional de Chile, Santiago, Chile, [8]NCALM, University of Houston, Houston, TX, USA

Abstract We show that a fixed smartphone network can provide robust Earthquake Early Warning for at least two orders of magnitude less cost than scientific-grade networks. Our software and cloud-based data architecture that we have constructed for the Alerta Sismica Temprana Utilizando Teléfonos Inteligentes (ASTUTI; Earthquake Early Warning Utilizing Smartphones) network in Costa Rica is easily scaled and exported. Implementation comprises provisioning and installing modern smartphones in judicious locations. Stand-up time for regionally operational networks can be on the order of days. We evaluated a non-parametric ground-motion detection and alerting strategy that would alert the entire Costa Rican population of any event with a ground motion detection threshold of 0.55–0.65 %g at four neighboring stations. During a 6-month evaluation period ASTUTI detected and alerted on five of 13 earthquakes with M_w 4.8–5.3 that caused felt Modified Mercalli Intensity shaking levels of 4.3–6. The system did not produce any false alerts and the undetected events did not produce wide-spread or significant felt shaking. System latencies were less than or similar to scientific-grade latencies. Alerts for all five detected events would have reached the capital city, San Jose, before strong *S*-wave shaking. This would have afforded time for Drop Cover Hold On actions by most residents. Two of the five alerts were triggered by *P*-waves suggesting that smartphone-based networks could approach the fastest theoretical EEW performance, especially with future expected improvements in smartphone sensors and processing algorithms.

Plain Language Summary We demonstrate that a network of smartphones deployed in fixed locations can provide Earthquake early warning (EEW) performance on par with scientific grade instrumentation at a fraction of the cost. This approach makes EEW accessible to resource-limited countries that may have not been to able to previously benefit from some form of EEW. In particular, combining the fixed-network smartphone sensors with a strategy targeting low cost of action protective measures such as Drop Cover Hold On could be very effective.

1. Introduction

Earthquake early warning's (EEW) fundamental promise is that earthquakes can be rapidly detected so that people and systems can be alerted to take protective action before shaking arrives at their location (Heaton, 1985). In order to maximize warning time and to minimize the population not receiving sufficient warning, EEW requires a dense sensor network so that earthquakes can be detected closest to wherever they may nucleate. The locations where earthquakes nucleate and where people reside, however, might be quite removed from one another. This requirement for dense sensor networks combined with the high cost of expensive scientific-grade sensors currently limits EEW systems to wealthy countries (Allen & Melgar, 2019). Alternatively, a new generation of low-cost accelerometer and geodetic sensors (Cochran, 2018) could make EEW generally accessible. In particular, utilizing smartphones, including via crowd-sourcing, is a potentially transformative way to provide EEW (Finazzi, 2016; Kong et al., 2016; Minson et al., 2015). Although

Received 9 FEB 2021
Accepted 24 MAY 2021

Author Contributions:

Conceptualization: Marino Protti, Todd Ericksen, Floribeth Vega, Elizabeth S. Cochran, Chris Duncan, Jon Avery, Sarah E. Minson, Esteban Chaves, Juan Carlos Baez, James Foster, Craig L. Glennie
Data curation: Marino Protti, Todd Ericksen, Floribeth Vega, Elizabeth S. Cochran, Chris Duncan, Jon Avery
Formal analysis: Marino Protti, Todd Ericksen, Julian Bunn, Elizabeth S. Cochran, Chris Duncan, Jon Avery, Sarah E. Minson, James Foster, Craig L. Glennie
Funding acquisition: Marino Protti, Todd Ericksen, Elizabeth S. Cochran, Sarah E. Minson, James Foster, Craig L. Glennie
Investigation: Marino Protti, Todd Ericksen, Julian Bunn, Floribeth Vega, Elizabeth S. Cochran, Chris Duncan, Jon Avery, Sarah E. Minson, Craig L. Glennie
Methodology: Marino Protti, Todd Ericksen, Julian Bunn, Floribeth Vega, Elizabeth S. Cochran, Chris Duncan, Jon Avery, Sarah E. Minson, Esteban Chaves, Juan Carlos Baez, James Foster, Craig L. Glennie
Project Administration: Marino Protti, Todd Ericksen, James Foster, Craig L. Glennie
Resources: Marino Protti
Software: Todd Ericksen, Julian Bunn, Elizabeth S. Cochran, Chris Duncan, Jon Avery, Sarah E. Minson, Craig L. Glennie
Supervision: Marino Protti, Todd Ericksen, Elizabeth S. Cochran, James Foster, Craig L. Glennie
Validation: Marino Protti, Todd Ericksen, Julian Bunn, Elizabeth S. Cochran, Chris Duncan, Jon Avery, Sarah E. Minson, Esteban Chaves, Juan Carlos Baez, James Foster, Craig L. Glennie
Visualization: Julian Bunn, Chris Duncan, Jon Avery, James Foster
Writing – review & editing: Marino Protti, Todd Ericksen, Julian Bunn, Floribeth Vega, Elizabeth S. Cochran, Chris Duncan, Jon Avery, Sarah E. Minson, Esteban Chaves, Juan Carlos Baez, James Foster, Craig L. Glennie

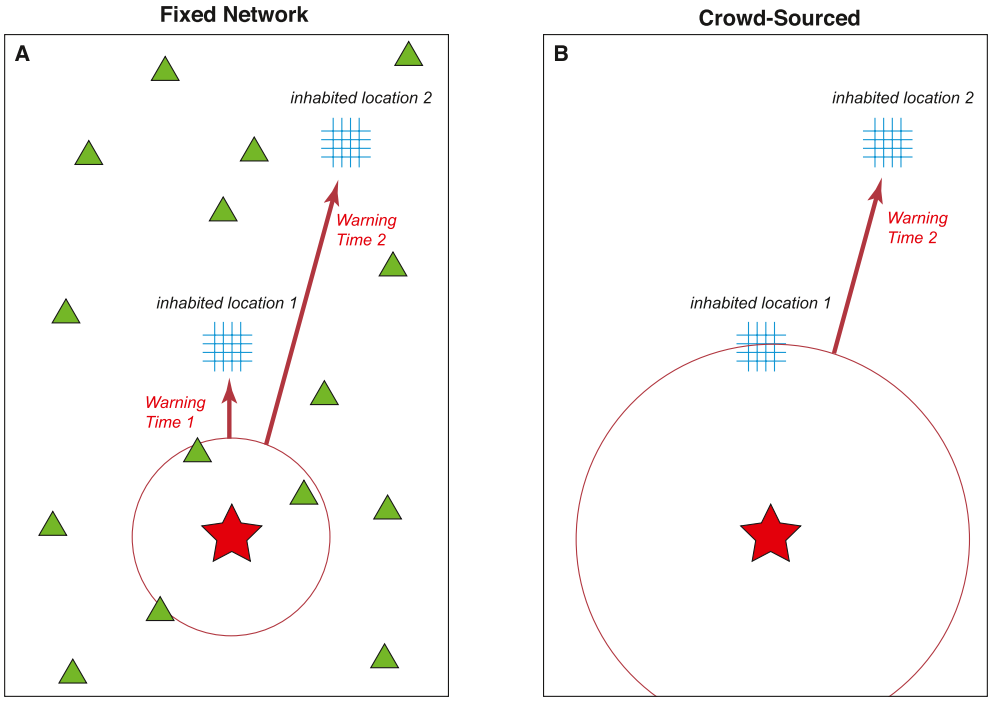

Figure 1. Cartoon depicting fixed-network (a) and crowd-sourced (b) earthquake early warning warning times for two population centers for a hypothetical earthquake (red star). The red circle indicates the time when the event is detected. With a fixed-network, the event is detected by nearby sensors located in zones of sparse population and both population centers could receive warning. With crowd-sourcing, the first population center's smartphones are used as the detectors and so it does not receive a warning. Moreover, the warning time for the second population center is less than what the fixed-network could have provided.

crowd-sourcing removes sensor cost from EEW budgets, it is fundamentally limited, in contrast to fixed networks, by sensors tending to be located in population centers rather earthquake source regions. With fixed networks, depending on the location of the event and the position of the sensors, all users could potentially get warnings (Figure 1a). By definition, however, some users in a crowd-sourced EEW system will never get warnings because it is their phones which are being used to detect the earthquakes (Figure 1b). Combining this detection advantage with the low capital and communications costs of smartphones may make fixed networks the optimal low-cost EEW configuration, perhaps even comparable to scientific grade systems. To the best of our knowledge, however, smartphone fixed network performance has never been examined. In this study, with a fixed network in Costa Rica, we demonstrate that judiciously placed smartphones can provide operational EEW for a country's population centers at a cost drastically reduced from, and at a performance level equivalent to, scientific grade instrumentation.

As with many techno-scientific advances with the potential for large societal impacts, the earliest projections of EEW system performance and its benefits to society have been modified and scaled back as EEW's theoretical, empirical, practical, and social limitations are better understood (Becker et al., 2020; McBride et al., 2019, 2020; Meier, 2017; Minson et al., 2018, 2019; Nakayachi et al., 2019; Trugman et al., 2019; Wald, 2020). To motivate and place in context our work, we review these recent developments, in particular as they pertain to smartphone-based EEW.

Ideally, an EEW system would issue actionable alerts prior to P (compressional)-wave arrival, affording the most time possible for protective actions. Even though a felt *P*-wave would hopefully serve as a natural EEW system alerting people to imminent shaking (Wald, 2020), site and path effects can preclude *P*-waves being felt ubiquitously, so a minimum criterion for an EEW system to be effective is for it to deliver alerts prior to the subsequent arrival of strongest shaking associated with *S*-waves. Currently, many operational EEW systems detect earthquakes using some permutation of point-source magnitude estimation from *P*-wave information (Chung et al., 2019). Point-source-based parameter estimation, albeit fast at initial detections,

exhibits degraded performance when events become large and magnitude estimates saturate (Hoshiba et al., 2010). Moreover, theoretical studies have recently found that the conventional EEW approach of using source parameters to forecast shaking causes alerts to be too slow for higher levels of shaking (Meier, 2017; Minson et al., 2018; Trugman et al., 2019), and to mostly produce missed and false alerts due to the intrinsic variability of ground motion (Gregor et al., 2014; Minson et al., 2019). Accordingly, EEW practitioners are developing ground-motion based approaches that issue alerts when one or more stations observe shaking above a threshold (Cochran et al., 2019; Kodera et al., 2018). For instance, by using strong ground motion that accrues sometime between *P*- and *S*-wave arrivals to directly forecast ground motion, alerts can be issued for strong shaking as soon as it is observed without having to wait for the rupture (and earthquake magnitude) to grow in size (Cochran et al., 2019; Kodera et al., 2018).

In addition to detection methodology, EEW alerting criteria are also quite variable. Alerting criteria are complicated by the simple physical fact that earthquake magnitude is not static; rather, it increases as an earthquake rupture evolves. The promise of EEW systems has been amplified by the idea that differences between the ways large and small earthquakes start could potentially be used to predict the final size of a growing earthquake, rather than relying on rapidly updating contemporaneous estimates of source parameters and ground motion (Melgar & Hayes, 2019; Olson & Allen, 2005). However, a growing number of studies have shown that the early *P*-wave holds little to no predictive power (Goldberg et al., 2019; Meier et al., 2017; Trugman et al., 2019). Furthermore, Minson et al. (2018) recently showed that given the velocities at which earthquake ruptures grow and seismic waves propagate, together with the exponential decay of ground-motion with distance from a propagating rupture, users' warning time for the strongest shaking will often be brief if EEW systems wait to issue alerts until earthquakes grow large enough that their forecast shaking is strong. Accordingly, it is becoming clear that EEW offers the most potential for successful mitigating actions, such as Drop-Cover-Hold-On (DCHO) (Porter & Jones, 2018) to be taken if alert thresholds are set at lower ground-motion levels than those expected to cause damage (Minson et al., 2018; Saunders et al., 2020).

Although an EEW system with low alert thresholds would likely produce alerts without significant shaking in some locations, the number of missed alerts would be minimized and the system would have the best chance of being effective during medium to larger events. For such a strategy to be successful, however, users must be more tolerant than is often assumed of receiving unnecessary alerts (the "Boy Who Cried Wolf" phenomena). Although there are essentially no studies explicitly addressing the "Boy Who Cried Wolf" phenomenon for EEW, other scientific communities with more established alerting relationships with users caution against the implicit assumption that user false alarm tolerance is low (Roulston & Smith, 2004). In fact, the small amount of evidence that exists suggests that EEW users may be false-alarm tolerant. Nakayachi et al. (2019), found from surveys associated with alerts from two Japanese events that, indeed, the user population was surprisingly tolerant of false alerts. Anecdotal surveys in Mexico found similar attitudes (Allen et al., 2018).

In this contribution, we implement the Alerta Sismica Temprana Utilizando Teléfonos Inteligentes (ASTUTI; Earthquake Early Warning Utilizing Smartphones) network in Costa Rica. For 6 months of continuous operation of the 82 station network, we assess a fixed smartphone network combined with a ground-motion based detection methodology. In order to focus on assessing smartphone EEW capability, we do not include any other data from Costa Rica's higher-grade seismic sensors (Moya-Fernández et al., 2020; Protti et al., 2014). We evaluate a low-threshold alert strategy that would alert the entire country upon the unambiguous detection of any earthquake, regardless of magnitude. The spatial distribution of events appears to be representative of the general spatial distribution of Costa Rican seismicity and allows us to examine system performance for events that occur within and outside of the network. Specifically, for each event, we quantify the percentage of Costa Rican population that would have sufficient warning time to undertake DCHO mitigating actions. Finally, all raw data collected for this project are freely available. As commercial entities with proprietary algorithm and data policies are poised to increase by orders of magnitude the number of smartphone EEW sensors and to issue public-safety alerts themselves (Stogaitis et al., 2020), we assert that it becomes ever more important that the scientific community have access to transparently collected and freely available smartphone data.

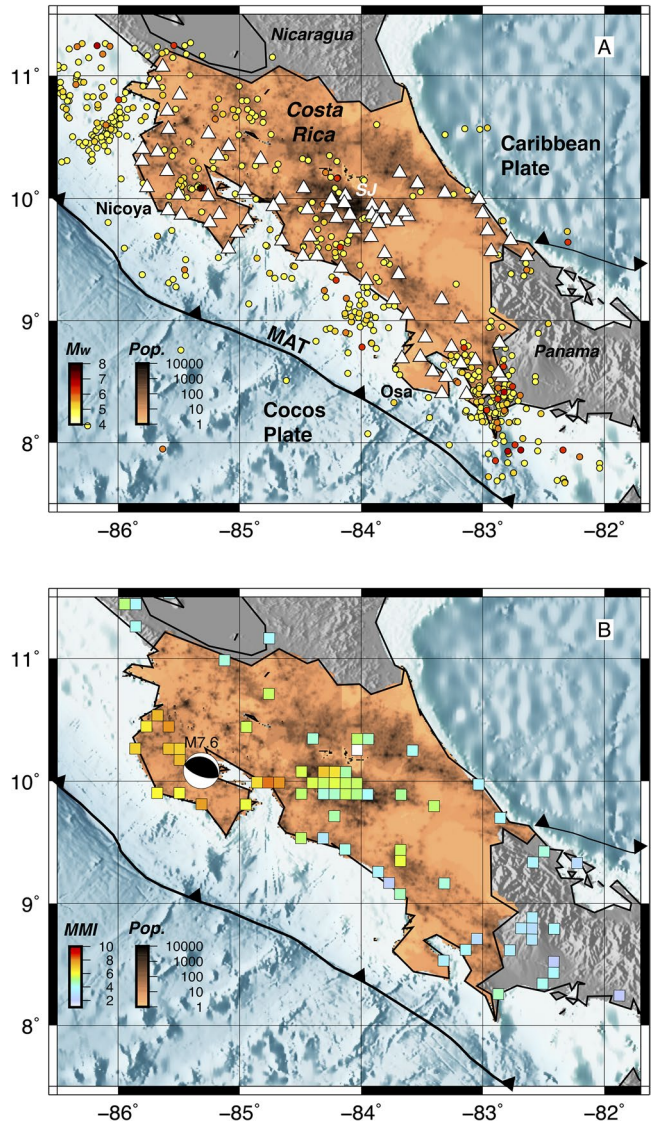

Figure 2. Costa Rica seismotectonic framework, population distribution, Alerta Sismica Temprana Utilizando Teléfonos Inteligentes; Earthquake Early Warning Utilizing Smartphones (ASTUTI) network, and the M7.6 2012 Nicoya peninsula earthquake. Basemap, WorldMap 1 km gridded population (copper colormap) and shaded topography and bathymetry (blue and gray colormaps). (a) Colored circles, earthquakes in the NEIC catalog from August 15, 2000 to June 3, 2020, colored by magnitude. White triangles, ASTUTI smartphone locations. MAT, Middle America Trench. SJ, San Jose city. (b) Beachball, focal mechanism of the 2012 Nicoya earthquake. Colored grid cells, Did You Feel It (DYFI) Modified Mercalli Intensity (MMI) values from the 2012 Nicoya earthquake.

2. Materials and Methods

2.1. System Design

Costa Rica's seismic hazard is due primarily, though not exclusively, to earthquakes generated by oblique subduction of the Cocos plate below the Caribbean plate at rates up to ∼8.5 cm/yr along the Middle America Trench (MAT) (DeMets et al., 2010; Protti et al., 2014; Figure 2**)**. In contrast to other subduction zones, MAT earthquakes in Costa Rica nucleate under the continent and not offshore (Protti et al., 2014). Since 1853, eight earthquakes greater than Mw 7.0 have occurred either on the northern Nicoya (1853, 1900, 1950, 2012) or southern Osa (1856, 1904, 1941, 1983) peninsulas (Kobayashi et al., 2014; Protti et al., 2014) The majority of Costa Rica's ∼5M population resides in the greater San Jose region, ∼60–200 km from the Pacific coast and principal seismogenic zone (Figure 2). For greater San Jose as well as Costa Rica's coastal regions, 10% expected peak ground acceleration (PGA) exceedance over the next 50 years is 0.55–0.90 g, in the upper ranges of global seismic hazard (Pagani et al., 2020). Recently, the Mw 7.6 2012 Nicoya peninsula earthquake was felt in the entire country, with PGA values as high as 0.5–1.4 g and MMI 5–7 reported in San Jose (Figure 2b). Generally, $M > 6$ events are felt country-wide.

Based on Costa Rica's seismotectonic framework and population distribution we designed the ASTUTI network with these principles: (a) Our EEW efforts are focused on warning people, not automated systems, and our targeted user response is DCHO. Because the cost of taking action for DCHO is so low, this implies that detection and alerting thresholds can be low. (b) We prioritize detecting and alerting for MAT earthquakes, the events that have the highest probability of affecting the largest percentage of the population, especially in San Jose. Although San Jose's central location exposes it to earthquake sources from the entire country, most non-MAT sources would be too close to San Jose to permit warnings. (c) If we wait to issue an alert until an event has grown large enough to cause shaking damage, then it will most likely be too late to issue actionable warnings (Minson et al., 2018; Trugman et al., 2019). Accordingly we attempt to issue warnings at the earliest detection of events of potential concern. (d) Because of local ground-motion variability (Minson et al., 2019) and because it is unlikely that earthquake ruptures are deterministic (Goldberg et al., 2019; Meier et al., 2017; Trugman et al., 2019) our detection and alerting is entirely non-parametric. In addition to making no attempt to estimate source information (such as location and magnitude), the alert does not include information about predicted ground-motion levels. (e) Based on the previous design principles, Costa Rica's generally small areal extent, and the country-wide shaking from MAT events such as the 2012 Nicoya event, we do not attempt to designate intra-country warning precincts; rather we evaluate the scenario where every alert will be issued for the entire country. (f) Because of the previous design priorities, there will likely be a number of alerts issued for smaller events when users will feel no shaking although an event was correctly detected. This will require rapid post-event messaging and constant user interaction and education to remind users that the system performed correctly even if they did not feel shaking (McBride et al., 2020). We stress, however, that, as of January 2021, we are not issuing public alerts, aside from those sent to our small group of beta testers. We leave thorough investigation of this topic to a future paper.

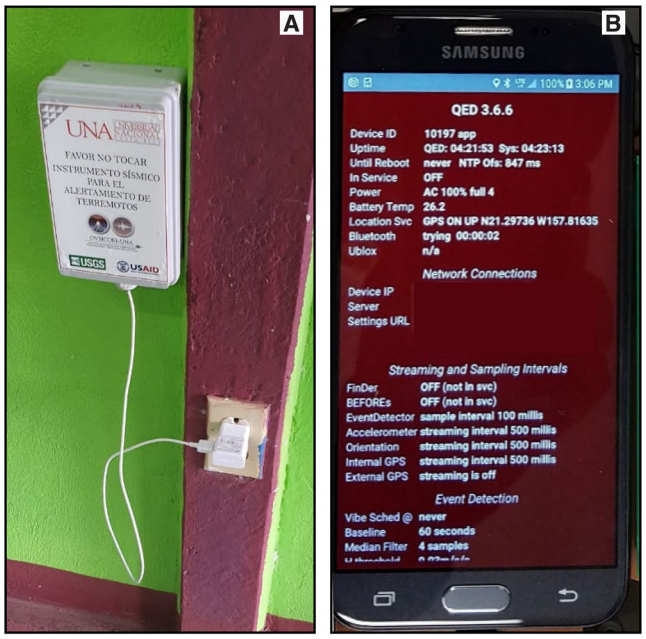

Figure 3. A typical Alerta Sismica Temprana Utilizando Teléfonos Inteligentes; Earthquake Early Warning Utilizing Smartphones station. (a) Photo showing the smartphone enclosure affixed to a wall. (b) Photo inside the enclosure of the smartphone screen showing the QED software application display.

2.2. Hardware, Network, and Data Architecture

From September to December 2019, we constructed the ASTUTI network (Figure 2a). For the duration of the testing period, the network comprised 82 stations. Closest to the MAT and most of the strongest expected sources, station spacing is ~30 km and it increases to 30–50 km away from the MAT. Higher station density closer to the subduction zone is similar to the configuration in Mexico (Cuéllar et al., 2017, 2018; Espinosa-Aranda et al., 2009; Suárez et al., 2018). Phones are installed on the ground floors of buildings in protective boxes and affixed to floors or walls (Figure 3). Previously, in addition to accelerometer data from smartphones, we have discussed and used GNSS, which typically requires outdoor installation (Minson et al., 2015). We found that many devices overheated, however, so for the initial phase of ASTUTI we made the operational decision to only employ phones installed on interior walls. Accordingly, the only data we use for ASTUTI are from on-board accelerometers. To date, our approach utilizes smartphones with the Android Operating System. Given that MEMs accelerometer performance in current model smartphones exceed performance metrics from those that had been previously tested in the field and on a shake-table (Kong et al., 2016; Minson et al., 2015), our criteria for phone choice included in-country availability and cost (Supporting Information).

Onboard the phones, our control and sensing software controls sensor sampling and logging, detects events, prepares data for use in various downstream processing algorithms, and sends data in short, labeled messages (Figure 4; Supporting Information). From December 2019 to late August 2020, phones streamed continuous data sampled at 10 Hz; subsequently we increased sampling rate for the entire network to its current rate of 100 Hz. At 100 Hz, data rate for each site is ~70–100 Mb/day. As of January 2021 we have collected more than 0.5 Tb of data (please see Acknowledgments, Samples, and Data section below for information on accessing the archived data).

2.3. Detection Algorithm and Alerting Strategy

Our detection algorithm is a modification of the ground-motion based Propagation of Local Undamped Motion algorithm (Kodera et al., 2018). In a polygonal mesh of station locations, we compensate for the noisier nature of smartphone accelerometers by requiring multiple neighboring stations to experience anomalous accelerations in order to trigger an alert. Here, we report on a quadrilateral mesh configuration of adjoining stations because we found an unacceptably large number of false alerts for triangular configurations. The station locations are organized into a set of unique, overlapping polygons whose sides are all less than a configurable length (currently 40 km). Once per second PGA values are measured at each station and the values are compared with a primary threshold (currently 0.6%g). If any station's PGA is above the threshold, the polygon it belongs to is marked as potentially triggered. The PGA values at each of the remaining stations in that polygon are compared with a secondary threshold (currently 0.55%g). If PGA values at all stations in a potentially triggered polygon are above the thresholds, an alert is issued. If not, the incoming PGA values continue to be monitored for up to 15 s (configurable), and the polygon will trigger if the remaining station PGA values rise above the secondary PGA threshold. Otherwise, the polygon times out, and no alert is triggered. Once a polygon is triggered, an alert is sent out using a cloud-based notification system (Amazon Web Services Simple Notification System). As of January 2021, alerts are only being sent to a small number of beta-subscribers in our research team.

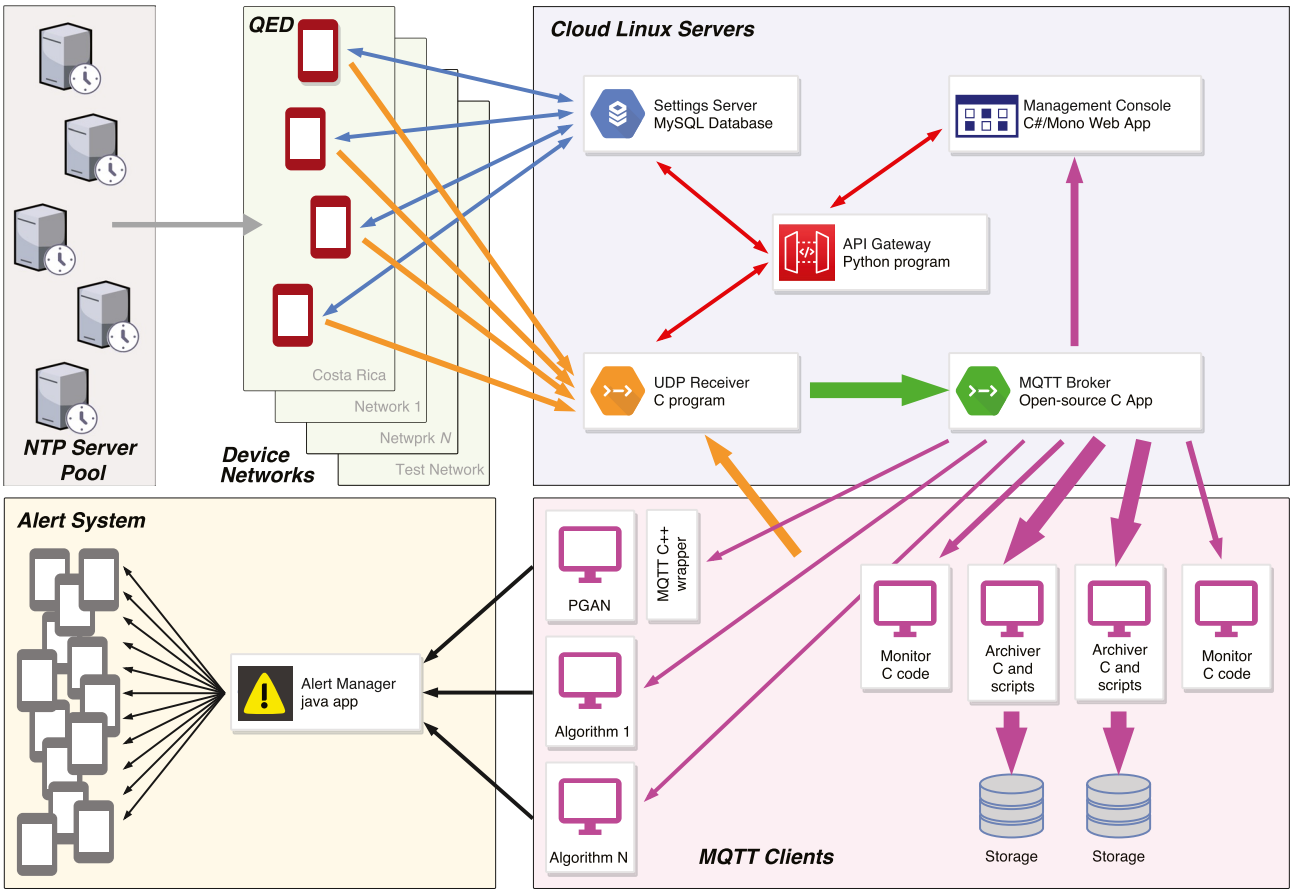

Figure 4. Schematic diagram of the Alerta Sismica Temprana Utilizando Teléfonos Inteligentes; Earthquake Early Warning Utilizing Smartphones approach. The general flow of alerting data and information is clockwise starts in the Device Networks box and end in the Alert System box. QED, "Quick Event Detection" smartphone software. NTP, network time protocol. UDP, user datagram protocol. MQTT, message queuing telemetry transport. API, application programming interface. MySQL, My structure queried language.

3. Data Quality and System Latency

We evaluated the system's data quality and latency during a 6 month period from December 2019 to June 2020. During this time, daily system up-time (defined as the percentage of each day the entire network was transmitting data) was consistently greater than 95%. After June 2020, as Covid-19 pandemic restrictions significantly limited travel in Costa Rica, we were not able to visit stations for routine or time-dependent site visits. Accordingly, station up-time and network coverage decreased during this period. In the Supporting Information section, we provide more details about system operation.

3.1. Data Quality

As with any seismic sensor, coupling to the ground and site-specific noise conditions control an individual phone's sensitivity. MEMS accelerometers in smart-phones have been shown to have the sensitivity to discriminate ground motions caused by earthquakes from background noise (Evans et al., 2014) even in crowd-sourcing scenarios where they may not be fixed in-place (Finazzi, 2016; Finazzi & Fassò, 2017; Kong et al., 2016; Kong, Patel, et al., 2019). In our fixed-network approach, phones are affixed to floors, baseboards, and walls in built structures, typically homes, schools, fire departments, hospitals, or municipal buildings (Figure 3). As such, they record accelerations through the filter of a structure emplaced in locally varying soil and/or rock substrate. This type of installation means that individual stations will record earthquakes (Figure 5a) as well as ambient non-seismic accelerations from myriad sources including road traffic, domestic motion, or thunder (Finazzi, 2020). In addition to site-specific noise, we have found that

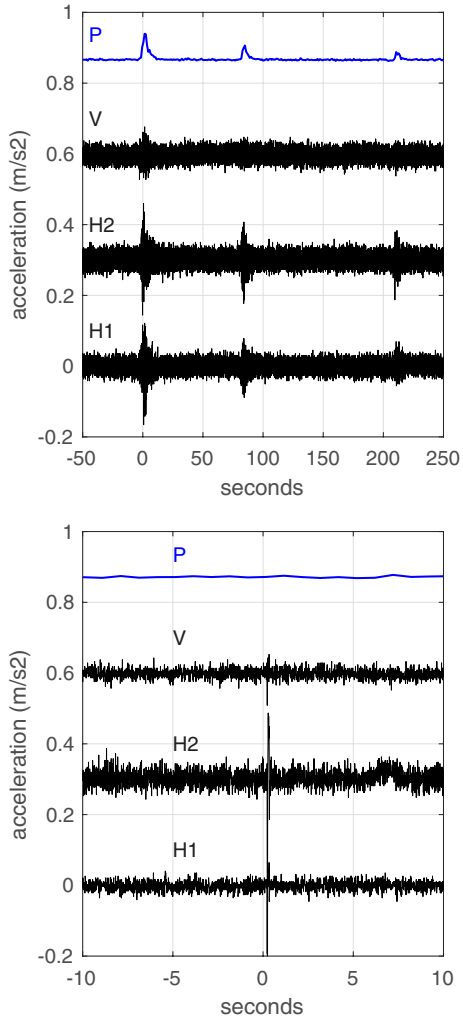

Figure 5. Examples of raw accelerometer and PGA data types from one station. Black, raw accelerometer data. V, vertical axis; H1, horizontal axis; H2, horizontal axis. Blue, P, processed PGA data message. (a) Example of how the PGA data type preserves the signal of 3 small earthquakes at 0, ~75 and ~210 s. (b) Example of how the PGA data type suppresses noise spikes at ~0 s.

some phones experience sporadic, unexplained, transient noise spikes, either on individual or multiple accelerometer components simultaneously (Figure 5b).

We combine the raw acceleration data from the three orthogonal accelerometers into a PGA data type (the "P" message) sampled and sent at 1 Hz. The data value is the vector norm of the individually de-meaned 100 Hz acceleration values and has units of m/s^2, also expressed as a percent of gravitational acceleration, %g. To mitigate transient noise spikes while permitting real seismic accelerations to pass, we implement a simple filter that takes the 30th percent highest value in a 1 s window (third highest if accelerometer sampling is 10 Hz, 30th highest if accelerometer sampling is 100 Hz; Figure 5b) (Kamigaichi et al., 2009).

Because the detection algorithm only requires exceedance of ground acceleration above a threshold, we characterize specific site and network data quality by examining histograms of PGA data. Generally, the entire network exhibits mean P-values of 0.25%g. Over periods of time varying from minutes to days, individual stations may experience elevated deviations from this background behavior (Figure 6). The causes of these transient periods of elevated background noise are varied and likely related to temporally changing site-specific noise such as local construction projects, changing traffic patterns, or persistent regional storms.

3.2. Latency Budget

Understanding and documenting the latency budget, along with assessing alert validity, is a critical aspect of EEW system operation. We define ASTUTI system latency, $\delta t_{latency}$, as the sum of three components $\delta t_{latency} = \delta t_{data} + \delta t_{detect} + \delta t_{alert}$ where δt_{data} is the time it takes for data to be transmitted from the phones and received by the hub, δt_{detect} is the time it takes for a given processing algorithm to detect an event, and δt_{alert} is the time it takes for a message to be received by a user after it has been sent by the processing algorithm. Of these, δt_{data} and δt_{alert} are only dependent on telecommunications factors and they are independent of the specifics of a given earthquake event. For different earthquakes, δt_{detect} depends on multiple factors including magnitude, rise-time, hypocentral location, near-source network geometry, and local site acceleration response. These factors will control the time it takes for seismic waves to travel from an earthquake to be sensed by a phone, the time it takes for a site to exceed detection thresholds, and the time it takes a particular algorithm to issue a detection.

From six months of continuously streamed data, we find that δt_{data} varies from 0.35 to 0.45 s depending on time of day; peak internet usage (early evening when people arrive home from work) also correlates with higher δt_{data} (Figure 7). For comparison, published δt_{data} for the Italian (Satriano et al., 2011), the Chinese (Zhang et al., 2016), and ShakeAlert (Cochran et al., 2018) EEW networks are 0.9, 2, and 1–3 s, respectively.

In order to robustly and simultaneously measure the real-time distribution of δt_{detect} and $\delta t_{alert,}$ as well as to test the full operation of the ASTUTI EEW system, we used smartphones' programmable vibration feature to cause the phones to shake at expected relative arrival times for a scenario earthquake. We use the M7.6 2012 Nicoya earthquake as a scenario event and program *S*-wave arrival time for each site calculating hypocentral distance (see methods) using a fixed move-out value for V_s of 3.2 km/s **(**Figure 8a**).** Each phone vibrated for ~10 s. Although they certainly do not reproduce the frequency nor amplitude content of real seismic waves interacting with built structures, smartphone vibrations are decent proxies for local earthquake accelerations in that they exceed the threshold values we use for earthquake detection at specified

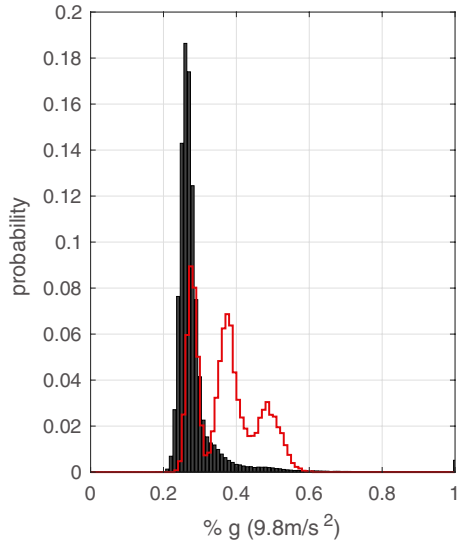

Figure 6. Histogram of PGA values for one station for one day (gray) and one hour (red). The current triggering threshold is 0.6%g.

times consistent with the earthquake rupture evolution and seismic wave propagation. Of course, the model of seismic wave propagation for the event could be more sophisticated but the constant V_s value is sufficient for the purpose of estimating average values of δt_{detect} and δt_{alert}. Note here we use S-wave arrival times to be conservative, but it is possible that trigger thresholds could be exceeded in the *P*-wave (see System Performance below).

Over a period of 3 days, we repeated the test, vibrating the phones on the Nicoya peninsula three times an hour at the M7.6 scenario relative times, resulting in a total of 216 simulations (Figures 8b and 8c). For this scenario, we find δt_{detect} has a mean value of ~12–13 s (Figure 8b). We measured δt_{alert} by sending text message alerts to a set of 15 people with cell phones in and around the greater San Jose region. We find mean value for δt_{alert} is ~4 s (Figure 8c). Because this is from a small number of phones that were relatively close together, it is not clear how representative this metric is of latencies that would occur when sending many thousands of alerts across a wider geographic region. Moreover, for widespread roll-out, push notification (Warren et al., 2014) is a more appropriate and lower-latency protocol than text messaging and development of this capability is occurring in the next phase of our work. For comparison we note, that in a recent test of ShakeAlert in San Diego county using the U.S. federal Wireless Emergency Alert (WEA) system (Minson et al., 2020), median δt_{alert} was ~13 s. To the best of our knowledge no other smartphone EEW projects have reported alerting latency data (Finazzi, 2016, 2020; Finazzi & Fassò, 2017; Kong et al., 2016, 2018, 2020; Kong, Inbal, et al., 2019; Kong, Patel, et al., 2019].

4. System Performance

4.1. Event Accuracy and Timeliness

We evaluate ASTUTI's performance in both detecting earthquakes and delivering alerts to people who would potentially experience shaking for a given earthquake, based on off-line playback from December 2019 to June 2020. We use Did You Feel It (DYFI) data to provide both a self-consistent metric and the most natural ground-truth for whether people in a given region experienced shaking (Atkinson & Wald, 2007).

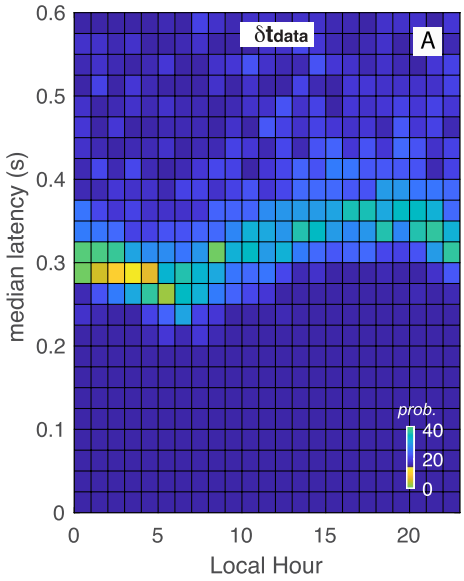

Figure 7. Hourly distribution of data latency, δt_{data}, for the 6 month observation period. Each column in the plot represents the median δt_{data} probability distribution function for an hour of the day.

During the period of assessment, we detected five of the 13 events that were accompanied by DYFI reports of shaking in Costa Rica (Figure 9). The majority of these events (9 of 13) occurred outside of the network, either offshore in the MAT or within Panama (Figure S1). Four of the detected events had thrust mechanisms and one had a strike-slip mechanism and they ranged in magnitude from from M_w 4.8 to 5.3. Only one of the detected events (2020-03-07) had an epicenter entirely within the network (Figure 9d). Generally, the ASTUTI-detected events were accompanied by stronger shaking that was felt by much larger percentages of the population as defined by interpolated DYFI reports. The detected events had median and maximum MMI levels of 4.3 and 6 with 41% (median) of the population experiencing shaking. In contrast, the non-detected events had median and maximum MMI levels of 2.9 and 3.8 with 0.002% (median) of the population experiencing shaking.

For each detected event, in addition to the associated DYFI data we plot the estimated position of the *S*-wave front (assumed to be the front of peak shaking) at the time that the alert was issued (solid magenta circles in Figure 9). Detection times, δt_{detect}, ranged from 11-30 s (median 22 s, Table 1). The detection times compare well with other scientific grade

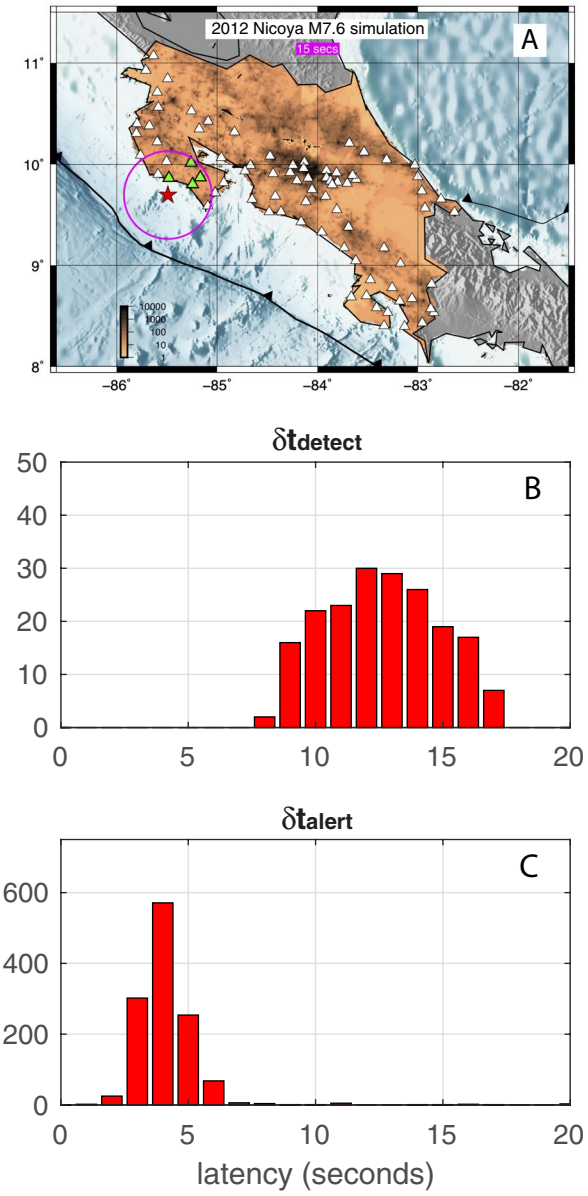

Figure 8. Alerta Sismica Temprana Utilizando Teléfonos Inteligentes; Earthquake Early Warning Utilizing Smartphones system latency and 2012 M7.6 Nicoya scenario vibration test. (a) Location map (as in Figure 2a) showing the 2012 M7.6 Nicoya scenario vibration test. Red star, epicenter. Magenta circle, *S*-wave position at the time, δt_{detect}, the time the event was detected. Green triangles, the stations that triggered the alert. (b) Histogram of time to detection, δt_{detect} for 216 vibrations tests. (c) Histogram of time to receipt of alert, δt_{alert}, for 216 vibration tests.

systems constructed and operated in similar seismic hazard settings, such as Cascadia and Mexico. For Cascadia, between 2019 and 2020 Shake Alert issued four alerts with δt_{detect} timing ranging from 8.3−13.9 s (ShakeAlertEventPage, 2020). Published δt_{detect} values from Mexico for three events range from 12-18 s (Cuéllar et al., 2018) and, although not explicitly presented, we estimate from data presented in a recent performance summary (Cuéllar et al., 2017) that minimum δt_{detect} is ∼8 s.

For each detected event we plot record sections of P messages and of the expected range of *P*- and *S*-wave velocities of 6 to 3 km/s, respectively (Figure 10). We find that two of the five events (December 8, 2019 and March 7, 2020, Figures 10a, 10b, 10g and 10h) triggered on the *P* wave, as shown by the magenta vertical line in the record sections. The three remaining events triggered with the *S*-wave. For all events aside from the one on 2020-03-07, ∼10 s elapsed between when the first and fourth stations surpassed the detection threshold. For the 2020-03-07 event, because this event was entirely within the network only 2 s elapsed between the first and fourth stations surpassing detection threshold.

4.2. Shaking

In addition to reporting the detection times we also assess the likely warning outcomes for population percentages (Tatem, 2017) for the case where the warning precinct for a detected event is the entire Costa Rican population (Figure 9). We interpolate the spatial distribution of DYFI reports to define an area of felt shaking, reasoning that it is likely ground-shaking occurred between sites of reported shaking (Cochran et al., 2019; Kodera et al., 2018). Although DYFI data contains uncertainty from humans' perceptional subjectivity (Goltz et al., 2020), we minimize this by applying a binary "shaking" or "no-shaking" classification to DYFI reports. We contend this is a conservative approach in that, for a given earthquake, the area of felt shaking represented by DFYI data is an under-rather than over-estimation: it seems more likely that people who felt shaking would not report it rather than that people would report felt shaking when none was felt. We categorize outcomes as True Positive-Shaking (TP-S): the system correctly detects an event and a user receives an alert prior to felt shaking; True Positive-No Shaking (TP-NS): the system correctly detects an event, a user receives an alert but does not feel shaking; No Alert (NA): the system correctly detects an event, but a user does not receive an alert prior to shaking; False Alert (FA): the system incorrectly detects an event and sends an alert, no shaking occurs anywhere; and Missed Alert (MA): a felt event occurs but the system does not issue an alert. Our MA definition permits a broad range of earthquakes to be counted, even those with source locations outside of the network and/or country. For this initial assessment, we prefer this more conservative MA definition. For each of these scenarios, to permit conservative evaluation of when users could expect to receive warning messages, in the plots we add to δt_{detect} 5 s, ∼1 s more than the median value of δt_{alert} from the vibration tests (see Section 3.2).

Over the 6 months of evaluation, 15.5%–71.0% of the population would have received TP-S outcomes, 27.1%–83% would have TP-NS outcomes and 1.5%–8.8% would have NA outcomes (Table 1). Outcomes can be grouped further according to onshore (in-network) and offshore (out-of-network) source categories. For the onshore events (12-8-19, 3-7-20, and 3-13-20) more time after warning is received is generally available because δt_{detect} is, on average, 10 s faster than the two offshore events (1-21-20a,b) and because the events

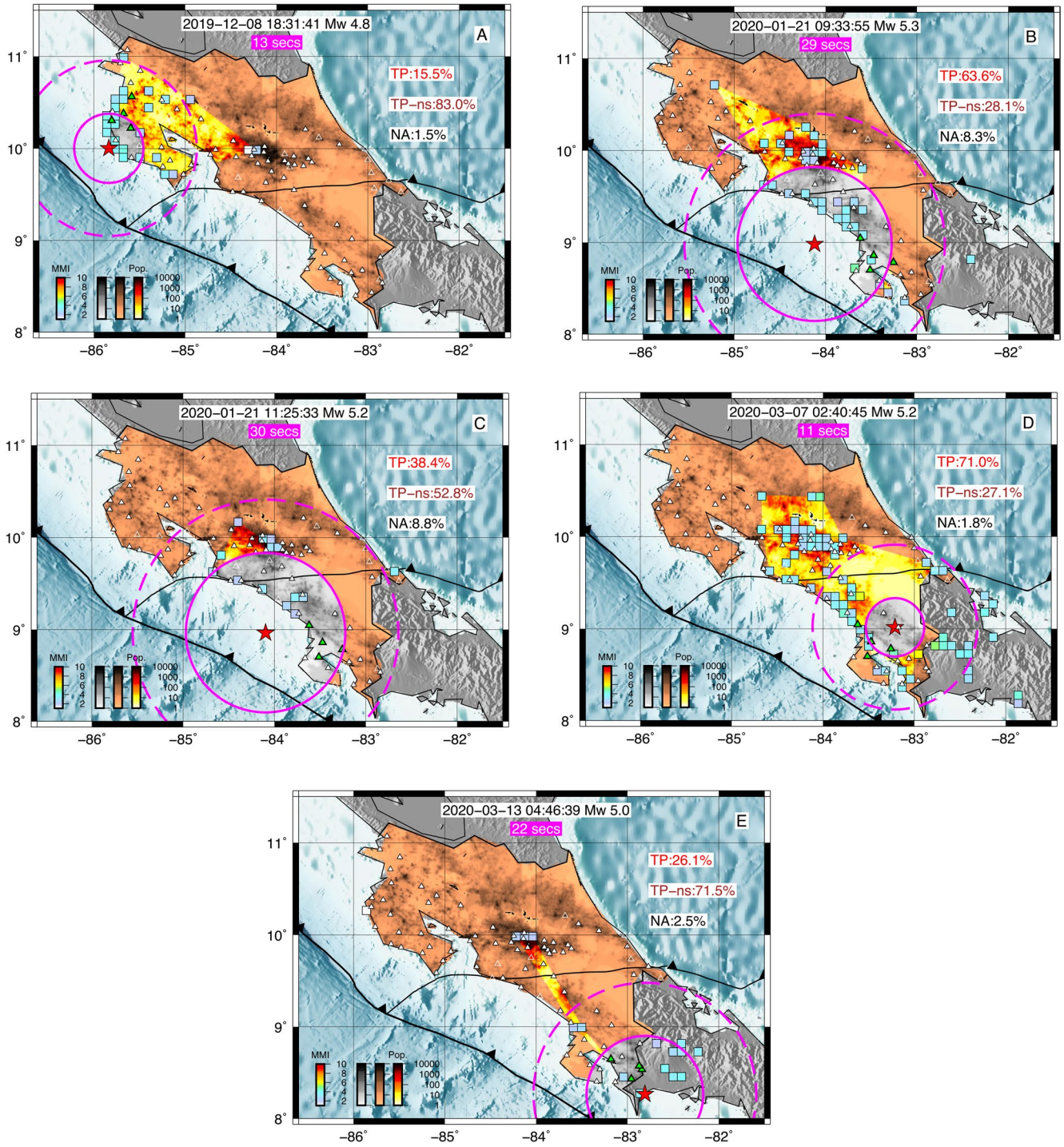

Figure 9. Alerta Sismica Temprana Utilizando Teléfonos Inteligentes; Earthquake Early Warning Utilizing Smartphones results from the five detected earthquakes demonstrating percentages of the population who would have experienced three different alerting outcomes: True-positive (TP-NS), True-positive no-shaking (TP-NS), and No-alert (NA). Each plot has the same symbology and nomenclature. Title with white box, origin time and magnitude of the event from OVSICORI. Magenta-box title, δt_{detect}. Magenta solid circle, estimated position of *S*-wave (3.2 km/s) at time δt_{detect}. Magenta dashed circle, estimated position of *S*-wave 20 s after time δt_{detect}. Twenty seconds represents ~5 s for alerting time, δt_{alert} (see Figure 6d) and 15 s for protective action such as Drop-Cover-Hold-On (DCHO). Green filled triangles, four stations that triggered the alert. White solid triangles, active stations at time of event. White empty triangles, inactive stations at time of event. Colored grid squares, DYFI cells. Hot population colormap, percentage of the population ("Pop.") that experienced True-positive (TP) outcomes. Copper population colormap, percentage of the population that experienced True-positive no-shaking (TP-NS) outcomes. Gray population colormap, percentage of the population that experienced No-alert (NA) outcomes. (a) December 12, 2019 M_w 4.8. (b) January 21, 2020a M_w 5.3. (c) January 21, 2020b M_w 5.2. (d) March 7, 2020 M_w 5.2. (e) March 13, 2020 M_w 5.0.

Table 1
Earthquakes in USGS NEIC Catalog From December 2019 to June 2020 That had Associated Did You Feel It (DYFI) Reports

Date	Time (UTC)	Lat. (deg)	Lon. (deg)	Depth (km)	Mw	MMI min	MMI max	MMI median	δtdetect (s)	TP-S (%)	TP-NS (%)	NA (%)
2019-12-08	18:31:42.871	10.1239	−85.794	35	4.8	1	4.3	3.3	13	16.5	83.1	0.4
2019-12-13	14:23:38.168	10.3837	−86.0839	36.25	4.6	2.2	2.2	2.2				
2019-12-24	00:25:09.970	10.8563	−86.4757	35	4.7	2	2.7	2.2				
2019-12-31	23:09:44.616	9.9422	−84.4593	59.75	4	2	2.7	2				
2020-01-21	09:33:56.399	9.043	−83.9471	11.06	5.3	2	4.8	3.1	29	66	29.3	4.7
2020-01-21	11:25:34.442	9.0071	−83.9595	11.02	5.2	2	3.8	2.7	30	40.7	54.6	4.6
2020-01-26	15:31:37.672	10.5928	−86.0141	24.8	4.4	1	2.2	1.6				
2020-02-03	10:29:55.598	10.6521	−86.0078	10	4.5	3.8	3.8	3.8				
2020-03-07	02:40:47.723	9.0114	−83.1647	39.22	5.2	2	6	3.4	11	71.4	27.2	1.4
2020-03-13	04:46:40.662	8.3099	−82.8384	19.17	5	1	3.9	2.7	22	26.1	72.1	1.8
2020-04-08	14:32:49.300	10.5208	−83.31	10	4.5	2	3.1	2.6				
2020-04-15	13:30:36.460	10.7398	−86.1658	41.62	5	2.5	3.7	3				
2020-04-17	09:34:35.051	9.3737	−84.1	49.46	4	2	3.6	2.8				

Notes. Date, event date; Time, event origin time; Lat., latitude; Lon., event longitude; Depth, event depth; M_w, moment magnitude; Alert, if an ASTUTI alert was triggered. See also Figures 7 and 8, and Figure S1. Date, origin date. Time, origin time (UTC). Lat, latitude; Lon., longitude; Depth, depth; M_w, moment magnitude; MMI min, minimum MMI from DYFI report; MMI max, maximum MMI from DYFI report; MMI median, median MMI from DYFI report. For the five detected events, additional outcomes are tabulated. δt_{detect}, time to detection; TP-S%, percent of population with True-positive outcomes. TP-NS%, percent of population with True-positive no-shaking outcomes. NA%, percent of population with No-Alert outcomes.

Abbreviations: ASTUTI, Alerta Sismica Temprana Utilizando Teléfonos Inteligentes; Earthquake Early Warning Utilizing Smartphones; MMI, Modified Mercalli Intensity.

on either the Nicoya or Osa peninsulas are far enough away from population concentrations (Figures 9a, 9d and 9e). The two off-shore events, however, yield the largest TP-S outcomes because Costa Rica's population is concentrated in and around the capital city, San Jose, near the center of the country and more than 100 km from these events (Table 1).

4.3. Missed & False Alerts

In order to analyze a self-consistent data set of felt shaking, we further classify MAs to be events for which the system did not produce an alert but that produced enough shaking for people to file DYFI reports. This is a minimum number as there may be other, smaller events that were felt but for which no DYFI reports were filed. During the period of evaluation there were 8 MAs with a range of M_w 4–5 (Table 1). Six of these were located well outside of the network (Figure S1). Of the remaining two, only one (12-31-2020, M_w 4) was located entirely within the network, the other (4-17-2020, M_w 4) was located on the Pacific coast at the edge of the network. For these events, less than 0.5% of the population reported shaking and the reported shaking never exceeded MMI 3 (Figure S1). These outcomes combined with the smallest detected event having M_w 4.8 (Table 1) suggest that the lower magnitude threshold for ASTUTI is currently somewhere between M_w 4 and 5. This is not, however, an absolute threshold as it is a function of station spacing and site specific ground-motion variability that requires a much longer time period of operation to accurately assess.

False alerts (FAs) can occur because of system glitches or non-seismic local or regional accelerations. From our time period of analysis we identified two types of system glitch sources that affected three or more neighboring stations nearly simultaneously. The first is unexpected phone vibration because of user error when programming the vibration tests. The second is regional power-grid instability causing AC electricity fluctuations that, in turn, cause multiple phones to unexpectedly vibrate simultaneously when they re-start as the regional AC power cycles off and on. Once they are identified, these are relatively straightforward FA sources to mitigate in real-time by better accounting of programmed vibrations and by identifying and excluding sites experiencing regional power cycling. The power-cycling issue is such an infrequent occurrence

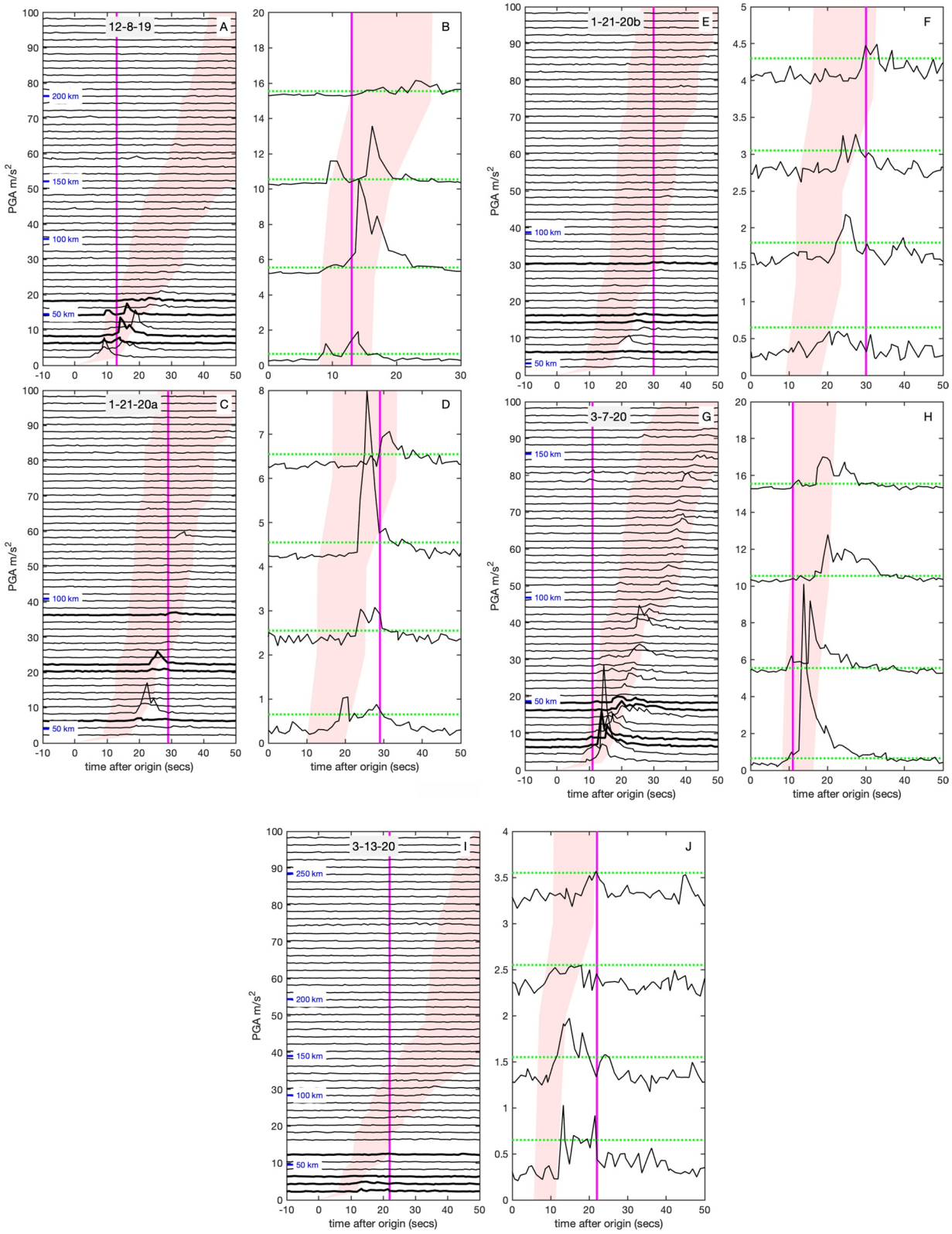
12-8-19
A
B
1-21-20b
E
F
1-21-20a
C
D
3-7-20
G
H
3-13-20
I
J
200 km
150 km
100 km
50 km
250 km
PGA m/s2
time after origin (secs)

Figure 10

that we do not believe any additional mitigation measures are required, though if it were to become more frequent, backup power aside from the phones' battery could be added. Real, non-earthquake accelerations from sources such as vehicles passing on the street, thunder shaking a structure, or people moving furniture near the phone installation are more difficult to mitigate. As the number of vertices in the triggering criteria is increased, the probability of regionally simultaneous non-seismic accelerations decreases. In our early tests, we found that it was necessary to include more than three stations in the detection algorithm to mitigate the effect of these types of unwanted accelerations on alert generation.

During the evaluation period, once system glitches were identified and noisy stations removed, we eliminated all FAs yielding a FA rate of 0%. This is similar performance to the result from offline runs on West Coast U.S. data of the ground-motion based algorithm from which ours is derived (Cochran et al., 2019). For further comparison, published FA rates for science-grade EEW networks range from 1 FA in 26 years for SASMEX (Suárez et al., 2018) to 2.5% in Taiwan (Xu et al., 2017) and 8% for Shake Alert (Kohler et al., 2020). The Japanese system reported many FAs after the 2011 M 9 Tohoku earthquake but to the best our knowledge has not published a FA rate (Hoshiba, 2014). For smartphone EEW, the Earthquake Network Project sets detection thresholds so that they do not exceed 1 FA per year, per country (Finazzi, 2020). This approach is a way to balance the often competing objectives of minimizing both MAs and FAs. The MyShake project has not yet reported a FA rate (Kong et al., 2020).

5. Discussion

Our work demonstrates that off-the-shelf smartphones deployed in a fixed network can provide operational EEW at performance levels similar to scientific grade networks but at a fraction of the cost. ASTUTI capital and annual costs are ~USD 22,000 and 20,000. For comparison, ShakeAlert capital and annual costs are ~USD 100 and 39 million (Given et al., 2018).

When normalized by population and area, ASTUTI's costs are more than two orders of magnitude less than ShakeAlert's (Supporting Information). The complete ASTUTI approach including smartphone software, cloud-based data and processing architecture, and field implementation is easily scaled and exported. Although we built ASTUTI over a period of months, this does not have to be the case. Phones can be provisioned and installed in the field within days or even hours in a rapid-response mode. Onces phones are provisioned and report to the cloud-based event hub, another instance of region-location specific processing can be initiated and regional EEW will be operational.

That two of the five detected events in the smartphone network were triggered by *P*-waves is an especially important finding, given that the fastest EEW performance possible is due to *P*-wave based detection (Chung et al., 2019; Cuéllar et al., 2018). Although ground-motion-based algorithms may be more likely to trigger on *S*-waves for moderate-sized events, there is no *a priori* requirement for this. Faster warnings could occur for larger events, such as the M_w 5.2 2020-03-07 event where P arrivals triggered the event and are seen in the records of many stations (Figure 10d). In fact, we identify *P*-waves in the acceleration records of individual stations for all five detected events (Figure 10). We expect *P*-wave EEW detection from smartphones to become more likely as future generation MEMs accelerometers become more sensitive and as algorithmic improvements, such as machine-learning detection (Kong, Inbal, et al., 2019), become operational.

It is ultimately peoples' response to, and perception of, an EEW system that determines its utility to a population. These are difficult to quantify characteristics and so, without direct user surveys, we must rely on inferences drawn from outcome statistics. Accordingly, it is notable that ASTUTI's 0% false alert rate is equivalent to or lower than all other EEW systems' reported FA rates. Our examination was only over six months, however, and so more operational time is required for a longer-term, more representative FA rate. Additionally, for the detected events, much larger percentages of the population (41% median) experienced

Figure 10. PGA, P-message, record section for the 5 detected earthquakes. Each plot has the same symbology, nomenclature, and scale. The left column shows all stations for a particular event, the right column shows a zoomed image of only the triggering stations. Stations are ordered with distance from the epicenter. Hypocentral distance shown in blue along the vertical axis. Triggering stations, thick black. Other stations, black. Triggering time, magenta line. Pink shading, ranges of 6 and 3 km/s for *P*- and *S*-wave arrival times, respectively. (a, b) December 12, 2019 M_w 4.8. (c, d) January 21, 2020a M_w 5.3. (e, f) January 21, 2020b M_w 5.2. (g, h) March 7, 2020 M_w 5.2. (i) March 13, 2020 M_w 5.0.

felt shaking. In contrast, for the non-detected events, much smaller percentages of the population (0.002% median) experienced felt shaking. Thus, ASTUTI detected and alerted for the events that appeared to "matter" to people (where "matter" is qualitatively identified here as earthquakes that caused enough shaking for people to submit DYFI reports). We suspect that this type of performance over a longer time period would foster user confidence and continued engagement with the EEW system, but this remains to be quantified by rigorous social science studies.

As expected, a low detection threshold criterion combined with a country-wide alerting region also led to significant population percentages where an alert would be received when no shaking was experienced (TP-NS outcomes). TP-NS percentage could be reduced by modifying alerting to include shaking estimation from source-parameter characterization and/or by imposing a more conservative magnitude threshold; these could potentially reduce user dissatisfaction from receiving unneccesary alerts. We suggest, however, that the benefit of attempting a more refined warning may be outweighed by the added variability associated with EEW parameter estimation and ground-motion prediction (Minson et al., 2018, 2019). Furthermore, it is not clear what penalty there might be in terms of user engagement if an EEW system provides alerts without felt shaking. We note that the general population may appreciate receiving an alert whenever an earthquake occurred, even if no one felt it (Nakayachi et al., 2019). Indeed, we are at the very early stages of studying the nuanced relationships between EEW system performance and human sentiment. Given this evolving understanding, a clear high-priority must be studying and refining EEW pre- and post-event education and messaging (McBride et al., 2020).

Our results support the notion that DCHO is an achievable EEW objective for concentrated population centers located far-enough away from earthquake sources. Times for people to undertake DCHO in two earthquake simulations were 5–30 s (McBride et al., 2019; Porter & Jones, 2018) whereas *S*-wave arrival in San Jose for the three onshore or near-shore events detected by ASTUTI was between ~30 and 50 s after median receipt of alert time (Figures 9a, 9d and 9e). For the other two detected offshore events (Figures 9b and 9c), the alert would have reached San Jose just before strong *S*-wave shaking, affording less time for DCHO. We note, however, that for two actual earthquakes, Nakayachi et al. (2019) report that taking no action was the most common outcome for people who received EEW alerts. This uncertainty highlights the often counter-intuitive nature of humans' interaction with automated warning systems and further stresses the importance of mitigation education and social science studies targeting DCHO activities.

Finally, as pointed out by others (Wald, 2020), updating construction codes and practices as well as promoting more widespread and thorough acceptance of simple mitigation actions such as DCHO deserve to be considered top priorities for earthquake-related resource allocation. The ASTUTI fixed network EEW approach is so inexpensive, however, that it need not interfere with other budgetary priorities for populations that do not have the resources to maintain advanced seismic networks but that could benefit from some form of EEW. Myriad implementation scenarios could be envisioned ranging from stand-alone smartphone networks to hybrid augmentations of preexisiting higher-grade instrumentation. Furthermore, the approach is so inexpensive that the sensing and detection benefits of judiciously placed sensors outweighs the even lower costs associated with crowd-sourcing. We note that in no way do we discount crowd-sourcing's value, especially the potential contribution to ground-motion and structural seismic response studies of massive numbers of crowd-source acceleration records (Kong et al., 2018).

Moreover, as digital home assistants become more ubiquitous, crowd-sourcing efforts (users permitting access to their personal devices) will move to fixed network modes. Especially for resource-limited populations, however, the day is still years away when user-contributed data will be spatially complete enough and temporally reliable enough to provide robust EEW capability for a larger population. With smartphone-based EEW in a nascent phase of rapid growth, we stress the need for continued scientific investigation and validation of these methodologies by the global community. Especially given the need for transparency when issues of public safety are concerned, we encourage open-access data policies for smartphone-based EEW systems.

6. Conclusions

We have demonstrated that a fixed-network of smartphones can provide operational Earthquake Early Warning at a cost that is at least two orders of magnitude less than scientific-grade networks. EEW performance metrics for the ASTUTI network compare well with scientific-grade networks, suggesting that stand-alone smartphone-based EEW could permit resource-limited populations to benefit from some form of EEW. The ASTUTI architecture is easily scaled, implemented, and exported. Network stand-up comprises simply provisioning smartphones, installing them in the field, and initiating a new location-specific instance of cloud-based processing. That two of five ASTUTI alerts were triggered by *P*-waves suggests that smartphone-based networks could approach the fastest theoretical EEW performance, especially with future expected improvements in smartphone sensors and processing algorithms. These type of lower cost sensors could also be deployed in hybrid networks to augment and complement more expensive scientific-grade sensors. ASTUTI's combination of ground-motion based detection with a country-wide alerting strategy demonstrates an effective EEW strategy for the common earthquake hazard setting where large population centers are close enough to be affected by large earthquakes but far enough away from them so that alerts may arrive in time to permit simple protective actions such as DCHO. ASTUTI's low detection threshold means that users would receive some alerts that are not accompanied by felt shaking. This may not be an impediment to user adoption of EEW systems, however; we strongly encourage more social science research targeting user's responses to various types of alerting schema employed by EEW systems.

Conflict of Interest

The authors declare no conflicts of interest relevant to this study.

Data Availability Statement

Data supporting the conclusions in this paper may be obtained at: http://ds.iris.edu/ds/nodes/dmc/forms/assembled-data/. Assembled data set number: 21-004; short name: ASTUTI.

Acknowledgments
We gratefully acknowledge USAID Bureau of Humanitarian Assistance for funding and especially Gari Mayberry for her oversight of this work since its inception. We thank Jeff McGuire, Annemarie Baltay, and Evelyn Roeloffs for earlier reviews of this manuscript and Chris Guillemot, Sarah McBride, David Wald, and Paul Earle for very interesting and helpful discussions. We thank the Associate Editor and 3 journal reviewers, in particular Dr. Gerardo Suarez, for their comments and suggestions which certainly improved the paper.

References

Allen, R. M., Cochran, E. S., Huggins, T. J., Miles, S., & Otegui, D. (2018). Lessons from Mexico's earthquake early warning system. *Eos, Earth and Space Science News*, *99*. https://doi.org/10.1029/2018eo105095

Allen, R. M., & Melgar, D. (2019). Earthquake early warning: Advances, scientific challenges, and societal needs. *Annual Review of Earth and Planetary Sciences*, *47*, 361–388.

Atkinson, G. M., & Wald, D. J. (2007). "Did You Feel It?" intensity data: A surprisingly good measure of earthquake ground motion. *Seismological Research Letters*, *78*(3), 362–368. https://doi.org/10.1785/gssrl.78.3.362

Becker, J. S., Potter, S. H., Vinnell, L. J., Nakayachi, K., McBride, S. K., & Johnston, D. M. (2020). Earthquake early warning in Aotearoa New Zealand: A survey of public perspectives to guide warning system development. *Humanities and Social Sciences Communications*, *7*(1), 1–12. https://doi.org/10.1057/s41599-020-00613-9

Chung, A. I., Henson, I., & Allen, R. M. (2019). Optimizing earthquake early warning performance: ElarmS-3. *Seismological Research Letters*, *90*(2A), 727–743. https://doi.org/10.1785/0220180192

Cochran, E. S. (2018). To catch a quake. *Nature Communications*, *9*(1), 2508. https://doi.org/10.1038/s41467-018-04790-9

Cochran, E. S., Bunn, J., Minson, S. E., Baltay, A. S., Kilb, D. L., Kodera, Y., & Hoshiba, M. (2019). Event detection performance of the PLUM earthquake early warning algorithm in Southern California. *Bulletin of the Seismological Society of America*, *109*(4), 1524–1541. https://doi.org/10.1785/0120180326

Cochran, E. S., Kohler, M. D., Given, D. D., Guiwits, S., Andrews, J., Meier, M.-A., et al. (2018). Earthquake early warning ShakeAlert system: Testing and certification platform. *Seismological Research Letters*, *89*(1), 108–117. https://doi.org/10.1785/0220170138

Cuéllar, A., Suárez, G., & Espinosa-Aranda, J. M. (2017). Performance evaluation of the earthquake detection and classification algorithm 2(tS–tP) of the Seismic Alert System of Mexico (SASMEX). *Bulletin of the Seismological Society of America*, *107*(3), 1451–1463. https://doi.org/10.1785/0120150330

Cuéllar, A., Suárez, G., & Espinosa-Aranda, J. M. (2018). A fast earthquake early warning algorithm based on the first 3 s of the P-wave coda. *Bulletin of the Seismological Society of America*, *108*(4), 2068–2079. https://doi.org/10.1785/0120180079

DeMets, C., Gordon, R. G., & Argus, D. F. (2010). Geologically current plate motions. *Geophysical Journal International*, *181*(1), 1–80. https://doi.org/10.1111/j.1365-246x.2009.04491.x

Espinosa-Aranda, J. M., Cuellar, A., Garcia, A., Ibarrola, G., Islas, R., Maldonado, S., & Rodriguez, F. H. (2009). Evolution of the Mexican seismic alert system (SASMEX). *Seismological Research Letters*, *80*(5), 694–706. https://doi.org/10.1785/gssrl.80.5.694

Evans, J., Allen, R. M., Chung, A., Cochran, E., Guy, R., Hellweg, M., & Lawrence, J. (2014). Performance of several low-cost accelerometers. *Seismological Research Letters*, *85*(1), 147–158. https://doi.org/10.1785/0220130091

Finazzi, F. (2016). The earthquake network project: Toward a crowdsourced smartphone-based earthquake early warning system. *Bulletin of the Seismological Society of America*, *106*(3), 1088–1099. https://doi.org/10.1785/0120150354

Finazzi, F. (2020). The earthquake network project: A platform for earthquake early warning, rapid impact assessment, and search and rescue. *Frontiers of Earth Science*, *8*, 243. https://doi.org/10.3389/feart.2020.00243

Finazzi, F., & Fassò, A. (2017). A statistical approach to crowdsourced smartphone-based earthquake early warning systems. *Stochastic Environmental Research and Risk Assessment*, *31*(7), 1649–1658. https://doi.org/10.1007/s00477-016-1240-8

Given, D. D., Allen, R. M., Baltay, A. S., Bodin, P., Cochran, E. S., Creager, K., et al. (2018). *Revised technical implementation plan for the ShakeAlert system—An earthquake early warning system for the West Coast of the United States* (Rep. 2331-1258). US Geological Survey.

Goldberg, D., Melgar, D., & Bock, Y. (2019). Seismogeodetic P-wave amplitude: No evidence for strong determinism. *Geophysical Research Letters*, *46*(20), 11118–11126. https://doi.org/10.1029/2019gl083624

Goltz, J. D., Park, H., Nakano, G., & Yamori, K. (2020). Earthquake ground motion and human behavior: Using DYFI data to assess behavioral response to earthquakes. *Earthquake Spectra*. https://doi.org/10.1177/8755293019899958

Gregor, N., Abrahamson, N. A., Atkinson, G. M., Boore, D. M., Bozorgnia, Y., Campbell, K. W., et al. (2014). Comparison of NGA-West2 GMPEs. *Earthquake Spectra*, *30*(3), 1179–1197. https://doi.org/10.1193/070113eqs186m

Heaton, T. (1985). A model for a seismic computerized alert network. *Science*, *228*, 987–990.

Hoshiba, M. (2014). Review of the nationwide earthquake early warning in Japan during its first five years. In Earthquake hazard, risk and disasters (pp. 505–529). Elsevier. https://doi.org/10.1016/b978-0-12-394848-9.00019-5

Hoshiba, M., Ohtake, K., Iwakiri, K., Aketagawa, T., Nakamura, H., & Yamamoto, S. (2010). How precisely can we anticipate seismic intensities? A study of uncertainty of anticipated seismic intensities for the Earthquake Early Warning method in Japan. *Earth Planets and Space*, *62*(8), 611–620. https://doi.org/10.5047/eps.2010.07.013

Kamigaichi, O., Saito, M., Doi, K., Matsumori, T., Tsukada, S. Y., Takeda, K., et al. (2009). Earthquake early warning in Japan: Warning the general public and future prospects. *Seismological Research Letters*, *80*(5), 717–726. https://doi.org/10.1785/gssrl.80.5.717

Kobayashi, D., LaFemina, P., Geirsson, H., Chichaco, E., Abrego, A. A., Mora, H., & Camacho, E. (2014). Kinematics of the western Caribbean: Collision of the Cocos Ridge and upper plate deformation. *Geochemistry, Geophysics, Geosystems*, *15*, 1671–1683. https://doi.org/10.1002/2014gc005234

Kodera, Y., Yamada, Y., Hirano, K., Tamaribuchi, K., Adachi, S., Hayashimoto, N., et al. (2018). The propagation of local undamped motion (PLUM) method: A simple and robust seismic wavefield estimation approach for earthquake early warning. *Bulletin of the Seismological Society of America*, *108*(2), 983–1003. https://doi.org/10.1785/0120170085

Kohler, M. D., Smith, D. E., Andrews, J., Chung, A. I., Hartog, R., Henson, I., et al. (2020). Earthquake Early Warning ShakeAlert 2.0: Public Rollout. *Seismological Research Letters*, *91*(3), 1763–1775. https://doi.org/10.1785/0220190245

Kong, Q., Allen, R. M., Kohler, M. D., Heaton, T. H., & Bunn, J. (2018). Structural Health Monitoring of Buildings Using Smartphone Sensors. *Seismological Research Letters*, *89*(2A), 594–602. https://doi.org/10.1785/0220170111

Kong, Q., Allen, R. M., Schreier, L., & Kwon, Y.-W. (2016). MyShake: A smartphone seismic network for earthquake early warning and beyond. *Science Advances*, *2*(2), e1501055. https://doi.org/10.1126/sciadv.1501055

Kong, Q., Inbal, A., Allen, R. M., Lv, Q., & Puder, A. (2019). Machine learning aspects of the MyShake global smartphone seismic network. *Seismological Research Letters*, *90*(2A), 546–552. https://doi.org/10.1785/0220180309

Kong, Q., Martin-Short, R., & Allen, R. M. (2020). Toward Global Earthquake Early Warning with the MyShake Smartphone Seismic Network, Part 1: Simulation platform and detection algorithm. *Seismological Research Letters*, *91*(4), 2206–2217.

Kong, Q., Patel, S., Inbal, A., & Allen, R. M. (2019). Assessing the sensitivity and accuracy of the MyShake smartphone seismic network to detect and characterize earthquakes. *Seismological Research Letters*, *90*(5), 1937–1949. https://doi.org/10.1785/0220180309

McBride, S. K., Becker, J. S., & Johnston, D. M. (2019). Exploring the barriers for people taking protective actions during the 2012 and 2015 New Zealand ShakeOut drills. *International Journal of Disaster Risk Reduction*, *37*, 101150. https://doi.org/10.1016/j.ijdrr.2019.101150

McBride, S. K., Bostrom, A., Sutton, J., de Groot, R. M., Baltay, A. S., Terbush, B., et al. (2020). Developing post-alert messaging for ShakeAlert, the earthquake early warning system for the west coast of the United States of America. *International Journal of Disaster Risk Reduction*, *50*, 101713. https://doi.org/10.1016/j.ijdrr.2020.101713

Meier, M.-A. (2017). How "good" are real-time ground motion predictions from earthquake early warning systems? *Journal of Geophysical Research: Solid Earth*, *122*(7), 5561–5577. https://doi.org/10.1002/2017jb014025

Meier, M.-A., Ampuero, J. P., & Heaton, T. H. (2017). The hidden simplicity of subduction megathrust earthquakes. *Science*, *357*(6357), 1277–1281. https://doi.org/10.1126/science.aan5643

Melgar, D., & Hayes, G. P. (2019). Characterizing large earthquakes before rupture is complete. *Science Advances*, *5*(5), eaav2032. https://doi.org/10.1126/sciadv.aav2032

Minson, S. E., Baltay, A. S., Cochran, E. S., Hanks, T. C., Page, M. T., McBride, S. K., et al. (2019). The limits of earthquake early warning accuracy and best alerting strategy. *Scientific Reports*, *9*(1), 2478. https://doi.org/10.1038/s41598-019-39384-y

Minson, S. E., Brooks, B. A., Glennie, C. L., Murray, J. R., Langbein, J. O., Owen, S. E., et al. (2015). Crowd-sourced global earthquake early warning. *Science Advances*, *1*(3), e1500036.

Minson, S. E., Meier, M.-A., Baltay, A. S., Hanks, T. C., & Cochran, E. S. (2018). The limits of earthquake early warning: Timeliness of ground motion estimates. *Science Advances*, *4*(3), eaaq0504. https://doi.org/10.1126/sciadv.aaq0504

Minson, S. E., Saunders, J. K., Bunn, J. J., Cochran, E. S., Baltay, A. S., Kilb, D. L., et al. (2020). Real-time performance of the PLUM earthquake early warning method during the 2019 M 6.4 and 7.1 Ridgecrest, California, Earthquakes. *Bulletin of the Seismological Society of America*, *110*(4), 1887–1903. https://doi.org/10.1785/0120200021

Moya-Fernández, A., Pinzón, L. A., Schmidt-Díaz, V., Hidalgo-Leiva, D. A., & Pujades, L. G. (2020). A strong-motion database of Costa Rica: 20 Yr of Digital Records. *Seismological Society of America*, *91*(6), 3407–3416.

Nakayachi, K., Becker, J. S., Potter, S. H., & Dixon, M. (2019). Residents' Reactions to Earthquake Early Warnings in Japan. *Risk Analysis*, *39*(8), 1723–1740. https://doi.org/10.1111/risa.13306%U

Olson, E. L., & Allen, R. M. (2005). The deterministic nature of earthquake rupture. *Nature*, *438*(7065), 212–215. https://doi.org/10.1038/nature04214

Pagani, M., Garcia-Pelaez, J., Gee, R., Johnson, K., Poggi, V., Silva, V., et al. (2020). The 2018 version of the global earthquake model: Hazard component. *Earthquake Spectra*, *36*(1_suppl), 226–251. https://doi.org/10.1177/8755293020931866

Porter, K., & Jones, J. (2018). How many injuries can be avoided in the HayWired Scenario through earthquake early warning and drop, cover, and hold on. In The HayWired earthquake scenario: US geological survey scientific investigations report—2017-5013 (pp. 401–429). USGS.

Protti, M., González, V., Newman, A. V., Dixon, T. H., Schwartz, S. Y., Marshall, J. S., et al. (2014). Nicoya earthquake rupture anticipated by geodetic measurement of the locked plate interface. *Nature Geoscience*, *7*(2), 117–121. https://doi.org/10.1038/ngeo2038

Roulston, M. S., & Smith, L. A. (2004). The boy who cried wolf revisited: The impact of false alarm intolerance on cost–loss scenarios. *Weather and Forecasting*, *19*(2), 391–397. https://doi.org/10.1175/1520-0434(2004)019<0391:tbwcwr>2.0.co;2

Satriano, C., Elia, L., Martino, C., Lancieri, M., Zollo, A., & Iannaccone, G. (2011). PRESTo, the earthquake early warning system for southern Italy: Concepts, capabilities and future perspectives. *Soil Dynamics and Earthquake Engineering*, *31*(2), 137–153. https://doi.org/10.1016/j.soildyn.2010.06.008

Saunders, J. K., Aagaard, B. T., Baltay, A. S., & Minson, S. E. (2020). Optimizing Earthquake Early Warning Alert Distance Strategies Using the July 2019 Mw 6.4 and Mw 7.1 Ridgecrest, California, Earthquakes. *Bulletin of the Seismological Society of America*, *110*(4), 1872–1886. https://doi.org/10.1785/0120200022

ShakeAlertEventPage. (2020). Retrieved from https://earthquake.usgs.gov/earthquakes/eventpage/us60007f42/executive; https://earthquake.usgs.gov/earthquakes/eventpage/uw61562126/executive; https://earthquake.usgs.gov/earthquakes/eventpage/nc73355700/executive; https://earthquake.usgs.gov/earthquakes/eventpage/nc73344735/executive

Stogaitis, M., Spooner, B., Robertson, P., Allen, R., Malkos, S., Gadh, T., et al. (2020). *Earthquakes at google, presented at 2020 Fall Meeting*. American Geophysical Union. Abstract S044-08.

Suárez, G., Espinosa-Aranda, J. M., Cuéllar, A., Ibarrola, G., García, A., Zavala, M., et al. (2018). A dedicated seismic early warning network: The Mexican Seismic Alert System (SASMEX). *Seismological Research Letters*, *89*(2A), 382–391. https://doi.org/10.1785/0220170184

Tatem, A. J. (2017). WorldPop, open data for spatial demography. *Scientific Data*, *4*(1), 1–4. https://doi.org/10.1038/sdata.2017.4

Trugman, D. T., Page, M. T., Minson, S. E., & Cochran, E. S. (2019). Peak ground displacement saturates exactly when expected: Implications for earthquake early warning. *Journal of Geophysical Research: Solid Earth*, *124*(5), 4642–4653. https://doi.org/10.1029/2018jb017093

Wald, D. J. (2020). Practical limitations of earthquake early warning. *Earthquake Spectra*. https://doi.org/10.1177/8755293020911388

Warren, I., Meads, A., Srirama, S., Weerasinghe, T., & Paniagua, C. (2014). Push notification mechanisms for pervasive smartphone applications. *IEEE Pervasive Computing*, *13*(2), 61–71. https://doi.org/10.1109/MPRV.2014.34

Xu, Y., Wang, J. P., Wu, Y.-M., & Kuo-Chen, H. (2017). Reliability assessment on earthquake early warning: A case study from Taiwan. *Soil Dynamics and Earthquake Engineering*, *92*, 397–407. https://doi.org/10.1016/j.soildyn.2016.10.015

Zhang, H., Jin, X., Wei, Y., Li, J., Kang, L., Wang, S., et al. (2016). An earthquake early warning system in Fujian, China. *Bulletin of the Seismological Society of America*, *106*(2), 755–765. https://doi.org/10.1785/0120150143